Published online 14 December 2006 *Nucleic Acids Research, 2007, Vol. 35, No. 2* ***e13***
doi:10.1093/nar/gkl1054

Increasing the sensitivity of DNA microarrays by metal-enhanced fluorescence using surface-bound silver nanoparticles

Chandran R. Sabanayagam* and Joseph R. Lakowicz

Department of Biochemistry and Molecular Biology, Center for Fluorescence Spectroscopy, University of Maryland School of Medicine, 725 West Lombard Street, Baltimore, MD 21201, USA

Received August 23, 2006; Revised October 3, 2006; Accepted November 19, 2006

ABSTRACT

The effects of metal-enhanced fluorescence (MEF) have been measured for two dyes commonly used in DNA microarrays, Cy3 and Cy5. Silver island films (SIFs) grown on glass microscope slides were used as substrates for MEF DNA arrays. We examined MEF by spotting biotinylated, singly-labeled 23 bp DNAs onto avidin-coated SIF substrates. The fluorescence enhancement was found to be dependent on the DNA spotting concentration: below ~12.5 μM, MEF increased linearly, and at higher concentrations MEF remained at a constant maximum of 28-fold for Cy5 and 4-fold for Cy3, compared to avidin-coated glass substrates. Hybridization of singly-labeled oligonucleotides to arrayed single-stranded probes showed lower maximal MEF factors of 10-fold for Cy5 and 2.5-fold for Cy3, because of the smaller amount of immobilized fluorophores as a result of reduced surface hybridization efficiencies. We discuss how MEF can be used to increase the sensitivity of DNA arrays, especially for far red emitting fluorophores like Cy5, without significantly altering current microarray protocols.

INTRODUCTION

DNA microarray technologies have dramatically increased the efficiency of DNA resequencing. In comparison to the classical macroscopic DNA dot blot assays that use isotopic labeling of the target DNA, fluorescent labels allow probe features in the lower micrometer range to be detected, allowing high-density arrays that consist of upwards to 10^6 probe sequences on a single microscope slide. However, fluorescence imaging currently is not as sensitive as isotopic methods, mostly because the relatively short 'half-life' of a fluorophore (~seconds) compared to isotopic radiation (weeks–years) limits the total number of detectable photons. In general, improving the sensitivity of fluorescence assays involves increasing the total number of photons detected.

There are various unique strategies that are used to increase the sensitivity of DNA microarrays. One technique is to increase the target-probe hybridization efficiencies by functionalizing the glass surface with reactive dendrimers to immobilize the probes (1–4), rather than just 2D surface immobilization. This approach is attractive because the efficiency of DNA hybridization increases when the probes are further from the surface. Another strategy utilizes dendrimer probes that contain hundreds of dyes that increase fluorescence intensity (5). Because each dendrimer contains an equal number of fluorophores, the intensity maintains a linear relation with the target surface concentration.

In this report we present a novel approach to increasing the sensitivity of DNA microarrays by engineering the substrate to increase the fluorophores' radiative rates through metal-enhanced fluorescence (MEF). MEF is a phenomenon that occurs when fluorophores are within about 100 Å from noble metal nanostructures. The MEF effect is thought to be a result of surface plasmons induced by the incident light or by the excited fluorophores. Enhancements of 10- to 40-fold have typically been observed for common organic fluorophores, such as fluoresceins, rhodamines and cyanines (6–21), and also for inorganic fluorescent quantum dots and nanocrystals (22–27). The increased brightness has been attributed to two main effects. First, there is an increase in the local excitation field due to the metal nanostructures. Second, the excited fluorophores couple with the surface plasmons, which reduce the natural fluorescence lifetime by an order of magnitude or more (8–21). Decreasing the excited state lifetime enables the fluorophore to cycle faster between the excited and ground states, and thus increases its emissive rate. Furthermore, a reduction in lifetime also decreases the time available for intersystem crossing into the triplet state, which is where irreversible photobleaching is most likely to occur, especially in the presence of molecular oxygen. For fluorophores that emit in the visible and near infrared regions, silver is the most common choice of metal with a characteristic plasmon absorption peak in the range of 300–450 nm.

*To whom correspondence should be addressed. Tel: +1 410 706 7500; Fax: +1 410 706 8408; Email: chandran@cfs.umbi.umd.edu

The magnitude and wavelength of the plasmon peak are dependent on the average surface concentration of nanoparticles, as well as their sizes, shapes and spatial distribution (28–31).

We determined MEF using two different array formats. First, to avoid confusing effects from surface hybridizations with enhanced fluorescence, we prehybridized the probe and labeled target DNAs in solution, then arrayed them onto microscope slides. Then, to characterize a practical DNA array, the probe oligonucleotides were first arrayed onto the microscope slide, and then the entire slide was incubated in a solution containing the labeled target oligonucleotides.

MATERIALS AND METHODS

Fabrication of avidin-coated silver island film (SIF) substrates

Standard $1'' \times 4''$ microscope slides were first cleaned with piranha solution (H_2SO_4:30% H_2O_2:; 3:1), rinsed with water, incubated in 10 M NaOH for 5 min, rinsed with water, then dried with filtered air. Cleaned slides were silanated by incubating in 1% 3-mercaptopropyltrimethoxy silane (MPTS) in 95% methanol acidified with 1 mM acetic acid. After 30 min of silanization, the slides were sonicated in 95% ethanol for 2 min then dried with filtered air. SIFs were grown on the MPTS surfaces by reduction of Ag^+ in N,N-dimethylformamide (DMF). MPTS acts as an adhesion promoter via its sufhydryl group, which has strong affinity for silver. The slides were incubated in a freshly prepared solution of 10 mM $AgNO_3$ (Sigma–Aldrich Co.) in anhydrous DMF (Sigma–Aldrich Co.) for 18 h. During this incubation time the solution color changes from yellow to orange to deep brown. After incubation, the slides were sonicated twice for 2 min each in 95% ethanol and then dried with filtered air.

The sulfhydryl reactive biotin derivative, [N-(6-(biotinamido)hexyl)-3′-(2-pyridyldithio)-propionamide, 'biotin-HPDP', Pierce Biotechnology, Inc.] was attached to the surface by adsorption of its disulfide group onto the SIFs, and covalent attachment to the exposed MPTS via its pyridyldithiol group. The SIF substrates were incubated in 200 μM biotin-HPDP in 95% ethanol overnight. The slides were washed for 30 min in 95% ethanol then dried with filtered air. Avidin (NeutrAvidin, Pierce Biotechnology, Inc.) was immobilized onto the biotinylated slides by incubating with 0.05 mg/ml in water, and stored in this solution at 4°C. Prior to DNA arraying, the avidin-coated slides were washed for 30 min in water and then dried with filtered air. Spectral characterization of the SIFs was done on a ultraviolet (UV)-visible spectrophotometer (Hewlett Packard model 8453). For avidin-coated glass slides, the above procedure was used, omitting SIF deposition.

Oligonucleotides

Oligonucleotides were synthesized with an Applied Biosystems model 394 instrument and high-performance liquid chromatography (HPLC) purified at the University of Maryland School of Medicine Biopolymer/Genomics Core Facility. The probe oligonucleotide has the sequence: biotin-5′-TCCACACACCACTGGCCATCTTC-3′. The target oligonucleotides are complementary to the probe sequence and contained either a Cy3 or Cy5 fluorophore at their 5′ termini. Oligonucleotide concentrations were determined by the absorbance at 260 nm. Double-stranded constructs were formed by mixing equimolar concentrations of probe and target oligonucleotides in 10 mM Tris–HCl (pH 7.4), heating to 85°C, and slowly cooling to 20°C at a rate of 1°C per minute on a thermocycler (Amplitron II, Barnstead Thermolyne Corporation).

Arraying probe oligonucleotides on the avidin-coated substrates

Biotinylated single- and double-stranded DNAs were arrayed onto the avidin-coated slides using a hand held 8-pin spotter (V&P Scientific, Incorporated), producing probe spot sizes with an average diameter of 640 μm, vertical center-to-center spacing of 1.1 mm, and horizontal center-to-center spacing of 1.4 mm. The spotting solution was 10 mM Tris–HCl (pH 7.4). After arraying, the slide were immersed in buffer supplemented with biotin [1 M NaCl, 10 mM Tris–HCl (pH 7.4), 1 mM EDTA and 1 mM d-biotin] for 10 min to remove unbound probes. Biotin was added in this wash solution in order to saturate the unoccupied binding sites of avidin, thus preventing the 'streaking' of the excess probes outside of the print area. The arrayed probes were washed for 20 min in water and dried with filtered air.

For hybridization experiments, 2-fold serial dilutions (50 μM to 390 nM) of single-stranded biotinylated oligonucleotides were arrayed onto avidin surfaces. Three-hundred μl of a mixture of 500 nM Cy3-labeled target oligonucleotide and 500 nM Cy5-labeled target oligonucleotide was suspended in high salt STE buffer [1 M NaCl, 10 mM Tris–HCl (pH 7.4) and 1 mM EDTA] and deposited on the arrays. $1'' \times 3''$ clean coverslips were placed on top of the solutions, and the arrays were incubated for 2 h at 45°C in a humid chamber. The hybridized arrays were washed for 30 min in STE buffer, rinsed with water and dried with filtered air.

DNA array imaging

Two-color imaging was done on a Perkin-Elmer ProScan-Array instrument. Cy3 was excited with a 543 laser, and Cy5 was excited with a 633 laser. The resolution was set to 10 μm, with 100% excitation intensity and PMT settings of 40 and 47% for Cy5 and Cy3 channels, respectively. These settings produced peak pixel intensities of about 30 000 counts (arbitrary units), approximately half of the dynamic range of the instrument (16 bits). Each spot comprised of about 3200 pixels. The raw image was processed with a 3×3 median filter to remove high-frequency noise. Background counts were determined by regions outside of the probe print area. Spot analysis and quantitation was done with software provided by the manufacturer. For photostability studies, a 500×500 μm^2 area within one 12.5 μM probe spot was continually imaged. The total pixel intensity per image was calculated using code written in MatLab. Curve fittings of the intensity decays were performed with Igor Pro (Wavemetrics).

RESULTS

Characterization of SIFs

SIFs were grown on silanated slides from the reduction of Ag^+ ions by DMF (28,29). Silver ion reduction with DMF is much slower than the more commonly used Tollen's reaction, but produces more uniform surface coverage and less batch-to-batch variations in our hands. An 18 h incubation in 10 mM $AgNO_3$, produces surface-bound silver nanoparticles with average diameter of around 80 nm. An electron micrograph of the surface shows the nanoscale heterogeneity of the particles' sizes, shapes and spatial distributions (Figure 1A).

The interaction of light with noble metallic nanoparticles can be characterized by an extinction spectrum, a combination of the absorption and scattering properties of the particles. For MEF, a strong scattering component of the extinction at the fluorophore's absorption and emission wavelengths is desirable. For an ideal 100 nm diameter spherical silver nanoparticle, the peak scattering contribution coincides roughly with the peak of the extinction (31). However it must be kept in mind that for the case of our SIFs, the surface-bound nanoparticles are far from ideal spheres, and moreover are heterogeneous in size and produce far more complicated scattering/absorption spectra (31). Nonetheless, a general trend with these metallic nanoparticles (50–100 nm diameter) is that large scattering/absorption ratios exist at wavelengths near the peak extinction and longer. The average extinction spectrum of five SIF substrates taken at ten different locations each is presented in Figure 1C (open circle symbols). First, note the small variations in the spectra (determined from the standard deviation bars) obtained from multiple samples and locations, indicating uniform nanoparticle coverage at the macroscopic scale. Obtaining uniform spectra is essential for microarrays because MEF must be a constant factor at all the probe sites. The SIF spectrum shows a characteristic extinction peak at 420 nm. For reference, the absorption and emission spectra for Cy3 and Cy5 is given in Figure 1B. The peak absorption/emission occurs at 549/562 nm for Cy3 and 646/663 nm for Cy5. Because these dyes have strong absorption and emission red-shifted with respect to the SIF extinction peak, we would expect MEF, although we cannot quantitatively predict the extent of fluorescence enhancement from these spectra.

A disulfide-containing biotin derivative (biotin-HPDP) was absorbed onto the silver nanoparticles; the pyridyldithiol group also reacts with the exposed thiols present in the silane adhesion layer. The average spectrum of the biotinylated SIFs shows little change in the extinction spectrum (Figure 1C). Binding of avidin with the biotinylated SIFs however, produces a notable spectral change: the extinction peak is red-shifted from 420 to 500 nm and is increased from ~0.4 to 0.5 U. This large change in extinction is due to the change in refractive index at the SIF interface upon avidin binding, which alters the surface plasmon resonance of the metallic nanoparticles (32).

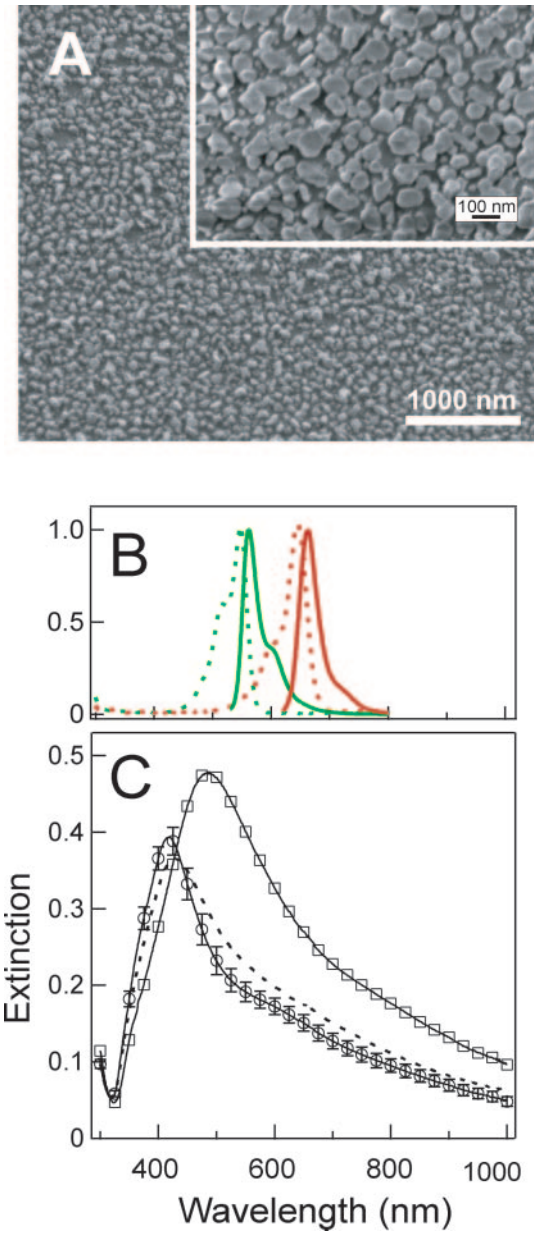

Figure 1. Physical and optical properties of the SIF grown on glass substrates. (**A**) The top image is a field emission scanning electron micrograph of the SIF showing the heterogeneity of the particles' shapes and sizes. The inset is a higher magnification of the SIF. (**B**) Normalized absorption spectra (dotted lines) and fluorescence spectra (solid lines) for Cy3 (green) and Cy5 (red) labeled double-stranded DNAs in solution. Cy3 was excited with 520 nm, and Cy5 was excited with 610 nm. (**C**) Visible extinction spectra for the SIF substrate at different steps during functionalization: SIF (circles); SIF-biotin (dashed line) and SIF-biotin-avidin (squares). Extinction spectra were taken with 1 nm resolution. The experimental errors were similar for the three spectra, but error bars are shown for only the case of bare SIF, for graphical clarity.

Metal-enhanced fluorescence of Cy3 and Cy5

MEF on SIFs was evaluated using a biotinylated 23 bp double-stranded DNA singly-labeled with Cy3 or Cy5 (Figure 2A). The duplex DNA was arrayed onto the slide with spotting concentrations ranging from 50 μM to 390 nM using 2-fold serial dilutions. Each concentration was spotted seven times to assess spot-to-spot variations. This spotting concentration pattern was additionally arrayed onto avidin-coated glass slides for comparison. Figure 3 shows plots of fluorescence intensity versus spotting

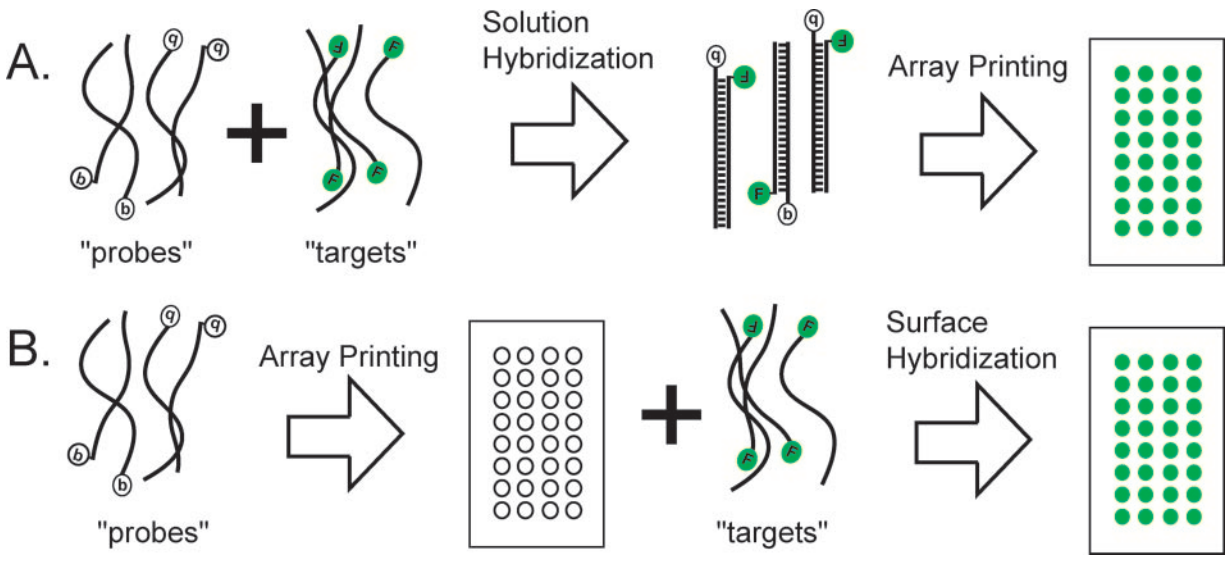

Figure 2. Scheme showing DNA hybridization in solution versus on a surface. (**A**) Solution hybridization. Biotinylated probe oligonucleotides 'b' and fluorophore-labeled target oligonucleotides 'F' are mixed in an equimolar ratio, heated to 85°C, then slowly cooled to form fluorescently-labeled double-stranded DNA. After cooling to room temperature, the DNAs are arrayed onto avidin-coated microscope slides. (**B**) Surface hybridization. Biotinylated probe oligonucleotides are arrayed onto avidin-coated microscope slides. Fluorophore-labeled target oligonucleotides are deposited onto the array surface for hybridization at 45°C.

concentration for the glass and SIF substrates. The adsorption kinetics of DNAs (short single- and double-stranded forms) onto solid surfaces can be modeled using the Langmuir adsorption isotherm:

$$\theta = \theta_{max} \frac{kC}{1 + kC},$$

where θ is the surface concentration of bound species, k represents an effective surface immobilization and C is the DNA probe spotting concentration (33). The amount of labeled DNAs bound to the surface is proportional to the fluorescence intensity, so the isotherm can be determined by substituting the background-corrected fluorescence for θ. The DNA binding data from glass fit very well to the Langmuir isotherm, with $k = 0.092\ \mu M^{-1}$ for both Cy3 and Cy5. For the SIF substrates, the isotherms deviate from the expected Langmuir form at low spotting concentrations, and show steeper concentration dependences (Figure 3), which we interpret as a surface concentration dependence of MEF. Above a critical surface concentration, fluorescence enhancement reaches a constant maximal value. The enhancement factor was calculated by dividing the background-subtracted SIF intensities by the corresponding glass intensities (Figure 3C). MEF was found to increase linearly up to a spotting concentration of about 12.5 μM. For higher DNA spotting concentrations, MEF is a constant maximum factor of about 28- and 4-fold for Cy5- and Cy3-labeled DNA, respectively. The difference in Cy5 versus Cy3 MEF is attributed to a higher red versus yellow wavelength scattering component of the plasmon extinction spectrum.

Photostability of fluorophores

The photostability of the bound duplex DNAs was determined by taking 200 consecutive scans of the same 500 × 500 μm^2 region within a 12.5 μm spotting concentration area (640 μm average diameter). Figure 4A and B show the results of the normalized intensities for Cy3 and Cy5 on glass and SIF substrates. The intensities of both fluorophores were found to decay faster on SIF as compared to glass. For glass, the intensity decays fit well to single exponential functions, with 1/e values of 520 ± 31 and 82 ± 1 scans for Cy3 and Cy5, respectively. This is consistent with Cy3 being a more stable fluorophore as compared to Cy5. For the SIF substrates, the normalized intensities were fitted to double exponential decays yielding 1/e values (amplitudes): 4.4 ± 0.1 (0.60) and 43 ± 1 (0.40) for Cy5 and 28 ± 0.6 (0.25) and 547 ± 8 (0.75) for Cy3. The double exponential intensity decays indicate that two photobleaching processes occur due to the presence of the SIF. These two processes most likely arise from the fluorophores on (or near) silver nanoparticles that exhibit enhanced fluorescence (fast decays), and fluorophores more distant from the nanoparticles, which show little or no enhanced fluorescence (slow decays). This interpretation is consistent with MEF being higher for Cy5 versus Cy3. For Cy5, the two decays due to the silver nanoparticles are both significantly faster than the decay on glass, suggesting enhancement of nearly all the fluorophores. Cy3 shows different behavior, with the slow intensity decay component on the SIF being similar to the decay on glass. We estimate that 25% of the Cy3 molecules on the SIF experience MEF, as determined from the amplitudes of the fits to the intensity decays.

The fluorophores on SIFs show faster intensity decays compared to glass substrates with similar scanning intensities. However, one should not interpret the faster decays presented in Figure 4A and B as a reduction of the dyes' photostabilities, because these plots represent normalized intensity decays. In order to accurately measure the affect of the SIFs on fluorophore photostability, one must carefully match the initial emissive rates before comparing their decay rates. In principle, the fluorescence intensities on

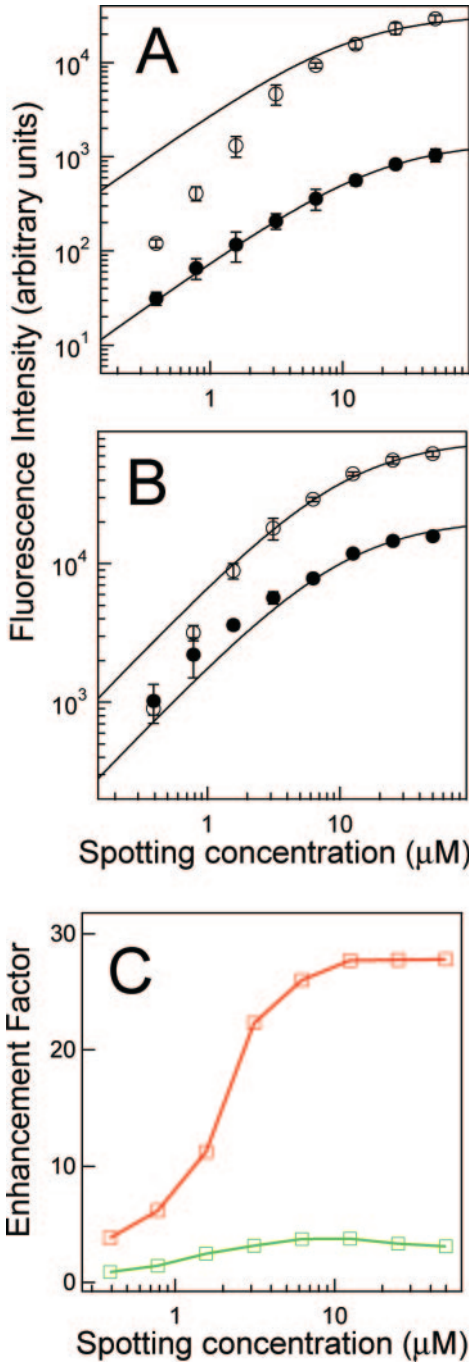

Figure 3. Solution hybridization. Intensity scans of Cy5- and Cy3-labeled double-stranded DNA arrayed onto SIF and glass substrates. Each data point represents an average of seven spots. Note the log scale on the *x*-axis. (**A**) Cy5 fluorescence on glass (filled circles) and SIF (empty circles). The solid lines are fits to Langmuir isotherms with $k = 0.092\ \mu M^{-1}$. (**B**) Cy3 fluorescence on glass (filled circles) and SIF (empty circles). Fits to Langmuir isotherms yielded similar k values as obtained with Cy5. (**C**) Plots of the intensity enhancement factor versus spotting concentration. Cy5 is shown in red, and Cy3 is shown in green. The enhancement factor was determined by dividing the average spot intensity of SIF with the corresponding glass values.

glass and SIF substrates can be equalized by adjusting the excitation power, but in practice it is much more difficult to realize because of the large difference in fluorescence intensities, which for Cy5 is 28-fold (Figure 3C). For instance, if one assumes a linear relation between excitation power and fluorescence, (which holds true if the fluorophores are not in saturating conditions), then the excitation source would need to be attenuated by a factor of 28 for the SIF substrate to produce similar emissive rates as observed for glass. A further experimental complication arises from the fact that the fluorophores are surface immobilized, and each scan will reduce the spot intensities as shown in Figure 4A and B. Therefore, determining the optimal excitation powers that equalizes the initial fluorescence intensities of the SIF and glass substrates is a non-trivial task. In order to compare the photostabilities of fluorophores on SIFs and glass, we instead plot the absolute cumulative intensities (under similar scanning intensities) versus scan number in Figure 4C and D. It can be easily seen that fluorophores on SIFs produce more detectable photons as compared with glass, and even after the last scan the cumulative amount of photons detected is about 2-fold and 5-fold higher on SIFs for Cy3 and Cy5, respectively. This is because the flux of emitted photons is much higher due to MEF. Assuming that the average total number of emitted photons per fluorophore is conserved, an increase in the radiative rate will decrease the half-life of the emitter. Thus, the increase in fluorophore stability on SIFs can be inferred indirectly from plots of the normalized intensity decays and absolute cumulative intensities for different initial emissive rates.

Hybridization to DNA arrays

A 2-fold serial dilutions (50 μM to 390 nM) of single-stranded probe oligonucleotides were arrayed onto avidin-coated glass and SIF substrates (Figure 2B). The DNA arrays were co-hybridized with 500 nM each of singly-labeled Cy3 and Cy5 complementary target oligonucleotides. This concentration of target oligonucleotides is in vast excess over the number of hybridization sites. After removal of non-hybridized DNA, the arrays were scanned on a two-color slide imager. Figure 5 shows a Cy5 scan for hybridization on glass and SIF substrates. It is interesting to note that the glass substrate produces the widely observed donut-shaped spot profile (e.g. see 6.25 μM and lower concentration rows in Figure 5), while this feature does not seem as prominent with SIF substrates. This donut or ring shape is a result of the mass transport of DNA towards the perimeter of the print area due to capillary flow during evaporation. A theoretical model that accurately describes ring deposits from evaporation has been discussed in detail and assumes: (i) the solvent droplet meets the (planar) surface at a non-zero contact angle; (ii) the contact line is pinned to its original position and (iii) the solvent evaporates (34). We speculate that the first two assumptions may not hold true for SIF substrates for the following reasons. If the silver nanoparticles protrude significantly from the surface, the resulting capillary flow will no longer be laminar, but turbulent, which may increase the overall DNA binding efficiencies in the interior of the printed spots. Also, the nanoparticles may cause the solvent to be pinned at multiple points within the print area, not just at the perimeter. For comparison, DNA arrays made by direct microcontact printing, a 'dry' method that does not involve droplet evaporation, yield uniform spots (35). Additionally, ring formation is not observed with

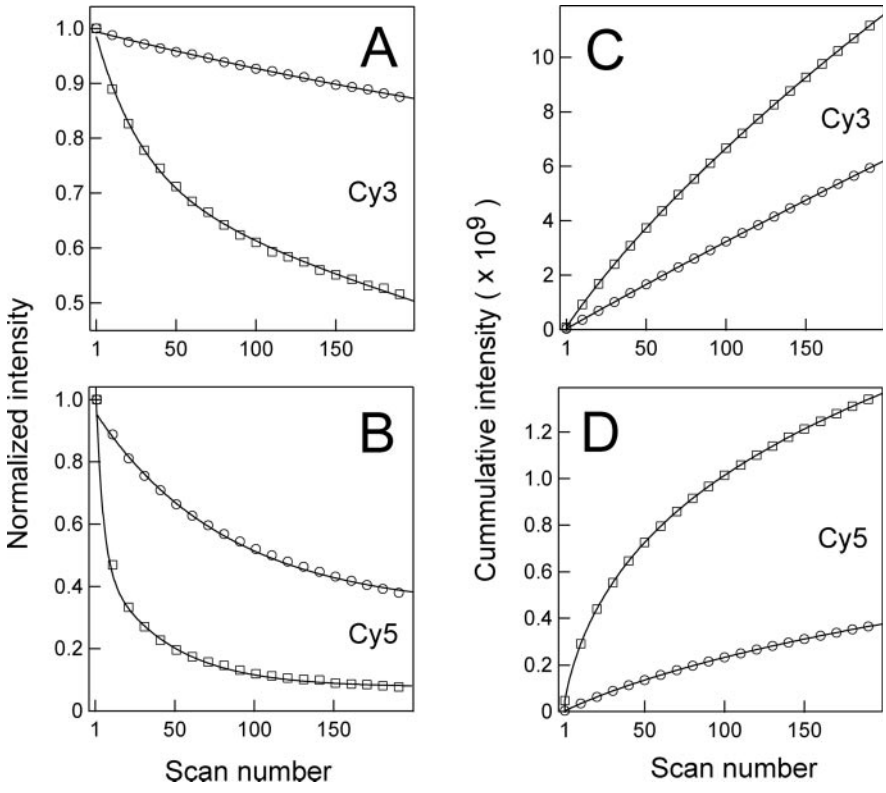

Figure 4. Photostability of Cy5- and Cy3-labeled duplex DNA arrayed onto SIFs and glass substrates. (**A**) Cy3 fluorescence on glass (circles) and SIF (squares). (**B**) Cy5 fluorescence on glass (circles) and SIF (squares). Solid lines are exponential fits to the data (see text). (**C**) Plots of the cumulative intensities of Cy3 versus the number of scans on glass (circles) and SIF (squares). (**D**) Plots of the cumulative intensities of Cy5 versus the number of scans on glass (circles) and SIF (squares). Symbols are shown for every 10th data point for graphical clarity.

oligonucleotide arrays fabricated by *in situ* synthesis (e.g. Affymetrix arrays).

Plots of intensity versus spotting concentration are given in Figure 6A and B. For both the glass and SIF substrates, the intensities of Cy3 and Cy5 reach a maximum between 6.25 and 12.5 μM, and then slowly decrease. The decrease in fluorescence is due to closely spaced probes at higher spotting concentrations that reduce the overall hybridization efficiency (36–39). Plots of the enhancement factor versus spotting concentration show that MEF is dependent on the surface concentration of fluorophores (Figure 6C), as was also observed for spotting prehybridized DNAs (Figure 3C). The maximum fluorescence enhancement was ~10-fold for Cy5 and 3-fold for Cy3. In comparing MEF for prehybridized DNAs versus surface hybridization, we note that there is a 2- to 3-fold decrease in fluorescence enhancement when hybridization is performed on a surface. The decrease in MEF is most likely due to a smaller percentage of fluorophores bound to the array, due to less efficient surface hybridization compared to bulk solution hybridization (39).

DISCUSSION

We have presented a novel application of MEF to increase the sensitivity of DNA microarrays. SIFs consisting of heterogeneous nanoparticles can support surface plasmons that interact with visible light. Fluorophores that are brought within close proximity (<100 Å) of surface plasmons experience high local excitation fields that increase their radiative rates and decrease their excited state lifetimes, resulting in higher fluorescence intensities. This enhancement phenomenon is very dependent on the spectral properties of the fluorophores. For the silver island substrates presented in this report, the characteristic extinction peak at ~500 nm yielded a maximum of 3-fold and 10-fold fluorescence enhancements with Cy3- and Cy5-labeled DNA targets co-hybridized onto microarrays. Additionally, MEF was also found to increase with surface concentration, and then saturates to a constant enhancement level. We note the difference in MEF when comparing Cy3 and Cy5 is due to the plasmonic properties of the SIF. The larger enhancement for Cy5 may occur because the scattering component of the extinction spectrum is stronger for the far red Cy5 emission (compare Figure 2B and C).

For studies in differential gene expression, two spectrally distinct fluorophores are used to determine the relative amounts of cDNAs synthesized from two sources (e.g. normal and diseased cells). Hence, adapting gene expression assays to benefit from MEF would involve using near infrared/infrared dyes, e.g. Cy5, Cy5.5 and Cy7 (Amersham), BODIPY and Alexa dyes (Molecular Probes), or IR700 and IR800 (LI-COR). Or, the surface plasmon absorption can be tuned for optimal MEF of fluorophores that emit in the visible region of the spectrum, by changing the silver nanoparticles' shapes and sizes. In general, decreasing the concentration of Ag^+ ions during silver reduction produces smaller nanoparticles that have their characteristic peak plasmon absorption blue-shifted compared to larger

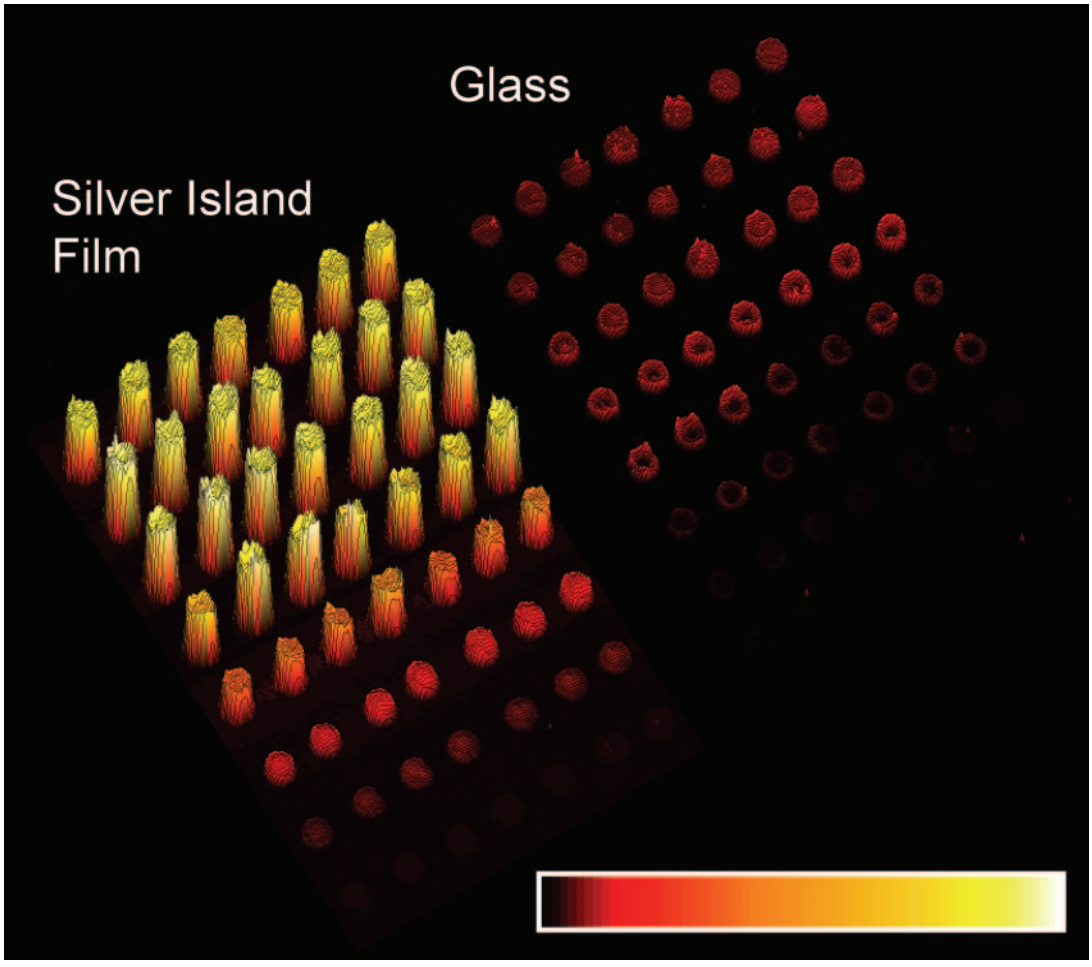

Figure 5. Fluorescence image of labeled oligonucleotide targets hybridized to MEF and glass DNA arrays. Probe oligonucleotides (23mer) were arrayed onto the substrates at different spotting concentrations: each row represents seven replicate spots at a given concentration; the rows are 2-fold serial dilutions starting with 50 μM (upper row). The image shows the Cy5 fluorescence as a result of co-hybridization with complementary Cy5- and Cy3-labeled targets (23mer). The scans were down sampled 5 × 5 pixels to plot the images in the figure, but for quantitation the original scan resolution (10 μm) was used (see Materials and Methods). The intensity bar shown in the lower right is a linear scale from 0 counts (black) to 34 000 counts (white).

nanoparticles. SIFs can also be created by thermal evaporation of silver metal (20), and the size and surface coverage of the nanoparticles can be controlled by the rate of evaporation and exposure time.

Enhancement factors as high as 4-fold for Cy3 and 28-fold for Cy5 were observed when the prehybridized DNAs were immobilized, which results in a higher concentration of labeled DNAs bound to the surface as compared to surface hybridizations. In principle, the enhancement factors for SIF surface hybridization can be increased by optimal spacing of the immobilized probes. Others have shown that the distance of the probes from the surface strongly affects DNA hybridization. The use of spacer molecules can reduce the steric interference of the surface on oligonucleotide hybridizations (36,40) or the length of the immobilized oligonucleotide probes can be increased from about 30 bases to 70 bases (41–43). Probe density also affects DNA hybridization efficiency. Earlier studies have shown that increasing oligonucleotide probe densities results in decreased hybridization efficiencies, likely due to electrostatic repulsion and steric factors (36). The results presented in Figure 6 show that above a critical surface probe concentrations (~12.5 μM), the fluorescence intensity decreases indicating less efficient hybridization, as observed by others.

The use of dendrimers has been explored as a method to immobilize oligonucleotide probes and increase hybridization efficiencies (1–4). The dendrimers act to distance the probes from the surface and into the bulk solution, and the probe spacing can be controlled by the properties of the dendrimer (e.g. number and length of branching segments). These technologies can be incorporated into SIF microarrays to optimize their performance. Dendrimers that contain hundreds of fluorophores have also been utilized as secondary probes for DNA arrays. Stears *et al.* (5) have shown a 16-fold increase in the detection sensitivity with dendrimers compared to linear probes. Again, the SIF DNA substrates are compatible with this technology, and their combination can potentially increase the sensitivity of DNA array assays even further.

The results presented in this report focused on the use of singly-labeled DNA targets. An interesting application of MEF DNA arrays is their use in the APEX (arrayed primer extension) assay. APEX is based on genotyping immobilized targets by using fluorescently-labeled dideoxynucleotide

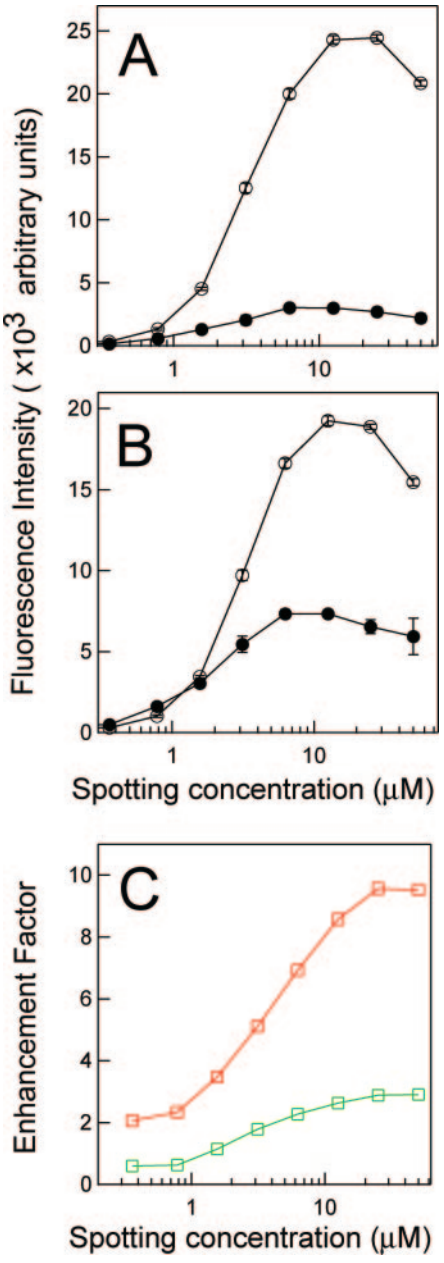

Figure 6. Surface hybridization. Intensity scans of Cy5- and Cy3-labeled target oligonucleotides hybridized to probes arrayed onto SIF and glass substrates. Note the log scale on the *x*-axis. (**A** and **B**) show the average intensity versus spotting concentration for Cy5 and Cy3, respectively, on SIF substrates (empty circles) and glass (filled circles). (**C**) Plots of the intensity enhancement factor versus spotting concentration from the hybridization data. Cy5 is shown in red, and Cy3 is shown in green.

triphosphates that are incorporated by DNA polymerase (44,45). The beauty of APEX lies in its ability to identify single-nucleotide polymorphisms in a parallel format. However, because the target is labeled with a single fluorophore, the method precludes the use of signal amplification, for example using highly-labeled dendrimer probes. Thus, MEF is an attractive approach to increase the sensitivity of APEX arrays, without significantly altering the assay.

In conclusion, we have utilized MEF to increase the fluorescence yield of DNA microarrays by as much as 28-fold for the near infrared Cy5 dye. The SIF substrates were found to be compatible with the high salt buffer and elevated temperature that are required for stringent target hybridization. Moreover, the silver nanoparticles were not damaged as a result of contact printing. Interestingly, with SIF substrates there is an absence of donut-shaped spots commonly seen with printed microarrays, and the fluorescence spots are much more uniform. Spot uniformity greatly improves microarray analysis because the spots are easier to identify and quantify by computer algorithms. Future work will focus on increasing the compatibility with the standard probe immobilization chemistries, namely covalent attachment of amine modified oligonucleotides to amine reactive silanes. The simplest method would involve depositing ~50 Å of SiO_2 on top of the SIF, then functionalizing the surface with silanes commonly used in microarray preparation. A 50 Å SiO_2 layer is comparable in dimensions to an avidin monolayer used in our current microarrays, and we would expect similar enhancement factors.

ACKNOWLEDGEMENTS

This work was supported by grants from the National Institutes of Health, RR08119 and HG002655. The Open Access publication charges for this article were waived by Oxford University Press.

Conflict of interest statement. None declared.

REFERENCES

1. Beier,M. and Hoheisel,J.D. (1999) Versatile derivatisation of solid support media for covalent bonding on DNA-microchips. *Nucleic Acids Res.*, **27**, 1970–1977.
2. Dolan,P.L., Wu,Y., Ista,L.K., Metzenberg,R.L., Nelson,M.A. and Lopez,G.A. (2001) Robust and efficient synthetic method for forming DNA microarrays. *Nucleic Acids Res.*, **29**, e107.
3. Benters,R., Niemeyer,C.M., Drutschmann,D., Blohm,D. and Wohrle,D. (2002) DNA microarrays with PAMAM dendritic linker systems. *Nucleic Acids Res.*, **30**, e10.
4. Le Berre,V., Trévisol,E., Dagkessamanskaia,A., Sokol,S., Caminade,A., Majoral,J.P., Meunier,B. and François,J. (2003) Dendrimeric coating of glass slides for sensitive DNA microarray analysis. *Nucleic Acids Res.*, **31**, e88.
5. Stears,R.L., Getts,R.C. and Gullans,S.R. (2000) A novel, sensitive detection system for high-density microarrays using dendrimer technology. *Physiol. Genomics*, **3**, 93–99.
6. Ritchie,G. and Burstein,E. (1981) Luminescence of dye molecules adsorbed at a Ag surface. *Phys. Rev.*, **24**, 4843–4846.
7. Glass,A.M., Liao,P.F., Bergman,J.G. and Olson,D.H. (1980) Interaction of metal particles with adsorbed dye molecules: absorption and luninescence. *Optics Letts.*, **5**, 368–370.
8. Weitz,D.A., Garoff,S., Hanson,C.D., Gramila,T.J. and Gersten,J.I. (1982) Fluorescent lifetimes of molecules on silver-island films. *Optics Letts.*, **7**, 89–91.
9. Lakowicz,J.R. (2001) Radiative decay engineering: biophysical and biomedical applications. *Anal. Biochem.*, **298**, 1–24.
10. Lakowicz,J.R., Shen,Y., D'Auria,S., Malika,J., Fang,J., Gryczynski,Z. and Gryczynski,I. (2002) Radiative decay engineering 2. Effects of silver island films on fluorescence intensity, lifetimes, and resonance energy transfer. *Anal. Biochem.*, **301**, 261–277.
11. Lakowicz,J.R. (2005) Radiative decay engineering 5: metal-enhanced fluorescence and plasmon emission. *Anal. Biochem.*, **337**, 171–194.
12. Malicka,J., Gryczynski,I., Fang,J., Kusba,J. and Lakowicz,J.R. (2002) Photostability of Cy3 and Cy5-labeled DNA in the presence of metallic silver particles. *J. Fluoresc.*, **12**, 439–437.
13. Malika,J., Gryczynski,I., Maliwal,B., Fang,J. and Lakowicz,J.R. (2003) Fluorescence spectral properties of cyanine dye labeled DNA

near metallic silver particles. *Biopolymers (Biospectroscopy)*, **72**, 96–104.
14. Malika,J., Gryczynski,I., Gryczynski,Z. and Lakowicz,J.R. (2003) Effects of fluorophore-to-silver distance on the emission of cyanine-dye-labeled oligonucleotides. *Anal. Biochem.*, **315**, 57–66.
15. Malika,J., Gryczynski,I., Fang,J. and Lakowicz,J.R. (2003) Fluorescence spectral properties of cyanine dye-labeled DNA oligomers on surfaces coated with silver particles. *Anal. Biochem.*, **317**, 136–146.
16. Malika,J., Gryczynski,I. and Lakowicz,J.R. (2003) Enhanced emission of highly labeled DNA oligomers near silver metallic surfaces. *Anal. Chem.*, **75**, 4408–4414.
17. Lakowicz,J.R., Malicka,J. and Gryczynski,I. (2003) (2003) Increased intensities of YOYO-1-labeled DNA oligomers near silver particles. *Photochem. & Photobio.*, **77**, 604–607.
18. Malicka,J., Gryczynski,I. and Lakowicz,J.R. (2004) Fluorescence spectral properties of labeled thiolated oligonucleotides bound to silver particles. *Biopolymers*, **74**, 263–271.
19. Zhang,J., Malika,J., Gryczynski,I. and Lakowicz,J. (2005) Surface-enhanced fluorescence of fluorescein-labeled oligonucleotides capped on silver nanoparticles. *J. Phys. Chem. B*, **109**, 7643–7648.
20. Zhang,J., Matveeva,E., Gryczynski,I., Leonenko,Z. and Lakowicz,J.R. (2005) Metal-enhanced fluoroimmunoassay on a silver film by vapor deposition. *J. Phys. Chem. B*, **109**, 7969–7975.
21. Lukomska,J., Malika,J., Gryczynski,I., Leonenko,Z. and Lakowicz,J.R. (2005) Fluorescence enhancement of fluorophores tethered to different sized silver colloids deposited on glass substrate. *Biopolymers*, **77**, 31–37.
22. Song,J.H., Atay,T., Shi,S., Urabe,H. and Nurmikko,A.V. (2005) Large enhancement of fluorescence efficiency from Cd/Se/ZnS quantum dots induced by resonant coupling to spatially controlled surface plasmons. *Nano Lett.*, **5**, 1557–1561.
23. Neal,T., Okamoto,K. and Scherer,A. (2005) Surface plasmon enhanced emission from dye doped polymer layers. *Opt. Express*, **13**, 5522–5527.
24. Lee,J., Govorov,A.O., Dulka,J. and Kotov,N.A. (2004) Bioconjugates of CdTe nanowires and Au nanoparticles: plasmon-exciton interactions, luminescence enhancement, and collective effects. *Nano Lett.*, **4**, 2323.
25. Lee,J., Govorov,A.O. and Kotov,N.A. (2005) Nanoparticle assemblies with molecular springs: a nanoscale thermometer. *Angew. Chem. Int. Ed.*, **44**, 7439.
26. Wang,Y., Li,M., Jia,H., Song,W., Han,X., Zhang,J., Yang,B., Xu,W. and Zhao,B. (2006) Optical properties of Ag/CdTe nanocomposite self-organized by electrostatic interaction. *Spectrochim. Acta A*, **64**, 101.
27. Ray,K., Badugu,R. and Lakowicz,J.R. (2006) Metal-enhanced fluorescence from CdTe nanocrystals: a single-molecule fluorescence study. *J. Am. Chem. Soc.*, **128**, 8998–8999.
28. Pastoriza-Santos,I. and Liz-Marzán,L.M. (2000) Reduction of silver nanoparticles in DMF. Formation of monolayers and stable colloids. *Pure Appl. Chem.*, **72**, 83–90.
29. Pastoriza-Santos,I., Serra-Rodríguez,C. and Liz-Marzán,L.M. (2000) Self-assembly of silver particle monolayers on glass from Ag+ solutions in DMF. *J. Colloid Interface Sci.*, **221**, 236–241.
30. Haynes,C.L. and Van Duyne,R.P. (2001) Nanosphere lithography: a versatile nanofabrication tool for studies of size-dependent nanoparticle optics. *J. Phys. Chem. B*, **105**, 5599–5611.
31. Sosa,I.O., Noguez,C. and Barrera,R.G. (2003) Optical properties of metal nanoparticles with arbitrary shapes. *J. Phys. Chem. B*, **107**, 6269–6275.
32. Riboh,J.C., Haes,A.J., McFarland,A.D., Yonzon,C.R. and Van Duyne,R.P. (2003) A nanoscale optical biosensor: real-time immunoassay in physiological buffer enabled by improved nanoparticle adhesion. *J. Phys. Chem. B*, **107**, 1772–1780.
33. Sabanayagam,C.R., Smith,C.L. and Cantor,C.R. (2000) Oligonucleotide immobilization on micropatterned streptavidin surfaces. *Nucleic Acids Res.*, **28**, e33.
34. Deegan,R.D., Bakajin,O., Dupont,T.F., Huber,G., Nagel,S.R. and Witten,T.A. (1997) Capillary flow as the cause of ring stains from dried liquid drops. *Nature*, **389**, 827–829.
35. Thibault,C., Le Berre,V., Casimirius,S., Trévisol,E., François,J. and Vieu,C. (2005) Direct microcontact printing of oligonucleotides for biochip applications. *J. Nanobiotechnology*, **3**, 7.
36. Schepinov,M.S., Case-Green,S.C. and Southern,E.M. (1997) Steric factors influencing hybridisation of nucleic acids to oligonucleotide arrays. *Nucleic Acids Res.*, **25**, 1155–1161.
37. Peterson,A.W., Heaton,R.J. and Georgiadis,R.M. (2001) The effect of surface probe density on DNA hybridization. *Nucleic Acids Res*, **29**, 5163–5168.
38. Georgiadis,R.M., Peterlinz,K.A. and Peterson,A.W. (2000) Quantitative measurements and modeling of kinetics in nucleic acid monolayer films using SPR spectroscopy. *J. Am. Chem. Soc.*, **122**, 3166–3173.
39. Gao,Y., Wolf,L.K. and Georgiadis,R.M. (2006) Secondary structure effects on DNA hybridization kinetics: a solution versus surface comparison. *Nucleic Acids Res.*, **34**, 3370–3377.
40. Guo,Z., Guilfoyle,R.A., Thiel,A.J., Wang,R. and Smith,L.M. (1994) Direct fluorescence analysis of genetic polymorphisms by hybridization with oligonucleotide arrays on glass supports. *Nucleic Acids Res.*, **22**, 5456–5465.
41. Hughes,T.R., Mao,M., Jones,A.R., Burchard,J., Marton,M.J., Shannon,K.W., Lefkowitz,S.M., Ziman,M., Schelter,J.M., Meyer,M.R. *et al.* (2001) Expression profiling using microarrays fabricated by an ink-jet oligonucleotide synthesizer. *Nat. Biotechnol.*, **19**, 342–347.
42. Relógio,A., Schwager,C., Richter,A., Ansorge,W. and Valcárcel (2002) Optimization of oligonucleotide-based DNA microarrays. *Nucleic Acids Res.*, **30**, e51.
43. Chou,C., Chen,C., Lee,T. and Peck,K. (2004) Optimization of probe length and the number of probes per gene for optimal microarray analysis of gene expression. *Nucleic Acids Res.*, **32**, e99.
44. Shumaker,J.M., Metspalu,A. and Caskey,T.C. (1996) Mutation detection by solid phase primer extension. *Human Mutat.*, **7**, 346–354.
45. Tõnisson,N., Zernant,J., Kurg,A., Pavel,H., Slavin,G., Roomere,H., Meiel,A., Hainaut,P. and Metspalu,A. (2002) Evaluating the arrayed primer extension resequencing assay of TP53 tumor suppressor gene. *Proc. Natl Acad. Sci. USA*, **99**, 5503–5508.